

Purification of Graphene Flakes by Using Radio-Frequency Thermal Ar Plasma

Jong Sik Oh¹, Ji Soo Oh¹, Myoung Sun Shin^{2,3}, Kyu Hang Lee^{2,3}, Jung Gil Kim^{2,3}, Sung Yong Choi², Seong In Kim², Se Han Lee⁴, Geun Young Yeom^{1,4,*}, and Kyong Nam Kim^{1,*}

¹Department of Materials Science and Engineering, Sungkyunkwan University, Suwon, Gyeonggi-do 440-746, South Korea

²Cheorwon Plasma Research Institute, Galmal-eup, Cheorwon-gun, Gangwon-do, South Korea

³Department of Electrical and Biological, Kwangwoon University, Wolgye-dong, Nowon-gu, Seoul, South Korea

⁴SKKU Advanced Institute of Nano Technology (SAINT), Sungkyunkwan University, Suwon, Gyeonggi-do 440-746, South Korea

ABSTRACT

In this study, graphene flakes (GFs) were treated with a radio-frequency thermal Ar plasmas, and the effect of the plasma treatment on the change of GF properties such as impurities, structural defects and morphology, and electrical properties was investigated. As the plasma treatment, two different rf powers of 27 kW and 17 kW were used and, as the GF feeding position, the up-state and the down-state relative to the plasma area were used. When the GFs were treated with the higher rf power and up-state, the impurities such as oxygen and sulfur in GFs were completely removed after one plasma treatment time while, when the GFs were treated with the lower rf power and down-state, the longer plasma treatment time of about three times was required to remove all the impurities. However, the higher rf power of 27 kW and the use of up-state increased the defects on the graphene surface possibly due to the more damage on the graphene surface by high temperature Ar plasma. By using the lower rf power of 17 kW and down-state, the removal of the impurities in GFs while decreasing (or, at least, without increasing) the structural defects on the graphene surface could be obtained. When the sheet resistance of the GFs treated with down-state 17 kW was measured, the decrease of sheet resistance of about 50% compared with that of the raw GFs could be observed while the GFs treated with other conditions of the higher rf power and up-state showed higher sheet resistances.

KEYWORDS: Plasma, Graphene Flakes, Impurities, Sheet Resistance.

1. INTRODUCTION

Graphene has been investigated enormously owing to the remarkable advantages such as high Young's modulus (~1,100 GPa), high thermal conductivity (~5,000 W m⁻¹ K⁻¹), high electron mobility (200,000 cm² V⁻¹ s⁻¹), large surface area (2,630 m² g⁻¹), etc.¹⁻⁹ These properties were obtained from the graphene fabricated by a mechanical cleavage method which was detached from graphite using a 3 M scotch tape.¹⁰ Even though the graphene obtained by the mechanical cleavage process shows high quality properties, but it is not a mass production method and not a large area process because the graphene less than tens of micro-meter is generally formed. For the fabrication of large area graphene, chemical vapor deposition (CVD) methods⁵⁻⁹ have been investigated but these methods generally require transferring from the growth

substrate to another substrate in addition to difficulty in mass production, therefore, the graphene obtained by these methods is very expensive for general purpose except for electronic device applications.

As inexpensive mass production methods, graphene fabrication methods such as chemical exfoliation method,¹¹⁻¹⁴ solvothermal synthesis method,^{15,16} and arc discharge method^{17,18} have been investigated and, by using these methods, graphene flakes (GFs) consisted of tens of micron size graphenes have been fabricated. Recently, these graphene flakes have been attracted a great deal of attention for potential applications such as composites,¹⁹⁻²² Li-ion batteries,²³⁻²⁵ supercapacitors,²⁶⁻²⁹ etc. However, the graphene fabricated these methods tends to be heavily decorated with oxygen-containing groups, and which degrades the graphene properties. Therefore, many researchers have investigated to remove oxide-containing groups using various reduction processes such as thermal reduction,^{30,31} chemical reduction,^{31,32} and microwave treatment.³³ The thermal reduction and chemical reduction processes can be done easily at a low cost but they require very high

*Authors to whom correspondence should be addressed.

Emails: gyyeom@skku.edu, knam1004@gmail.com

Received: 17 August 2014

Accepted: 14 February 2015

temperature (>2000 °C/min) and can cause environmental pollution, respectively, in addition to the difficulty in the mass-production. As another reduction process, plasma reduction methods have been also investigated to lower the processing temperature and to enhance the eco-friendliness but, currently have poor reduction rate.^{34,35}

In this study, as an approach to remove impurities on the graphene flakes (GFs) at large quantities, a radio frequency (rf) thermal plasma system has been investigated and the effect of graphene treatment with a high density inductively coupled plasma (ICP) on the removal of the impurities in the GFs was studied in addition to the change of structural defects and electrical properties as applications to the electrodes for general electrical devices.

2. EXPERIMENTAL DETAILS

Figure 1(a) shows the reactor where the graphene flakes are treated by rf Ar plasmas. The reactor is composed of a moveable GF feed tube, an Ar gas feed tube surrounding the GF feed tube, and an ICP source with a dielectric cylindrical chamber and a surrounding inductive antenna where the GFs are treated by the plasma while passing through the plasma from the top to bottom. As the GFs, the bulk graphene nanoplatelets purchased from a company (XGS-M15, XG Sciences) were used in the experiment. As the rf power to the ICP source, 17 kW and 27 kW of 4 MHz were used. The GF feed tube was positioned up-state or down-state relative to the plasma generated in the reactor to control the plasma treatment time and condition

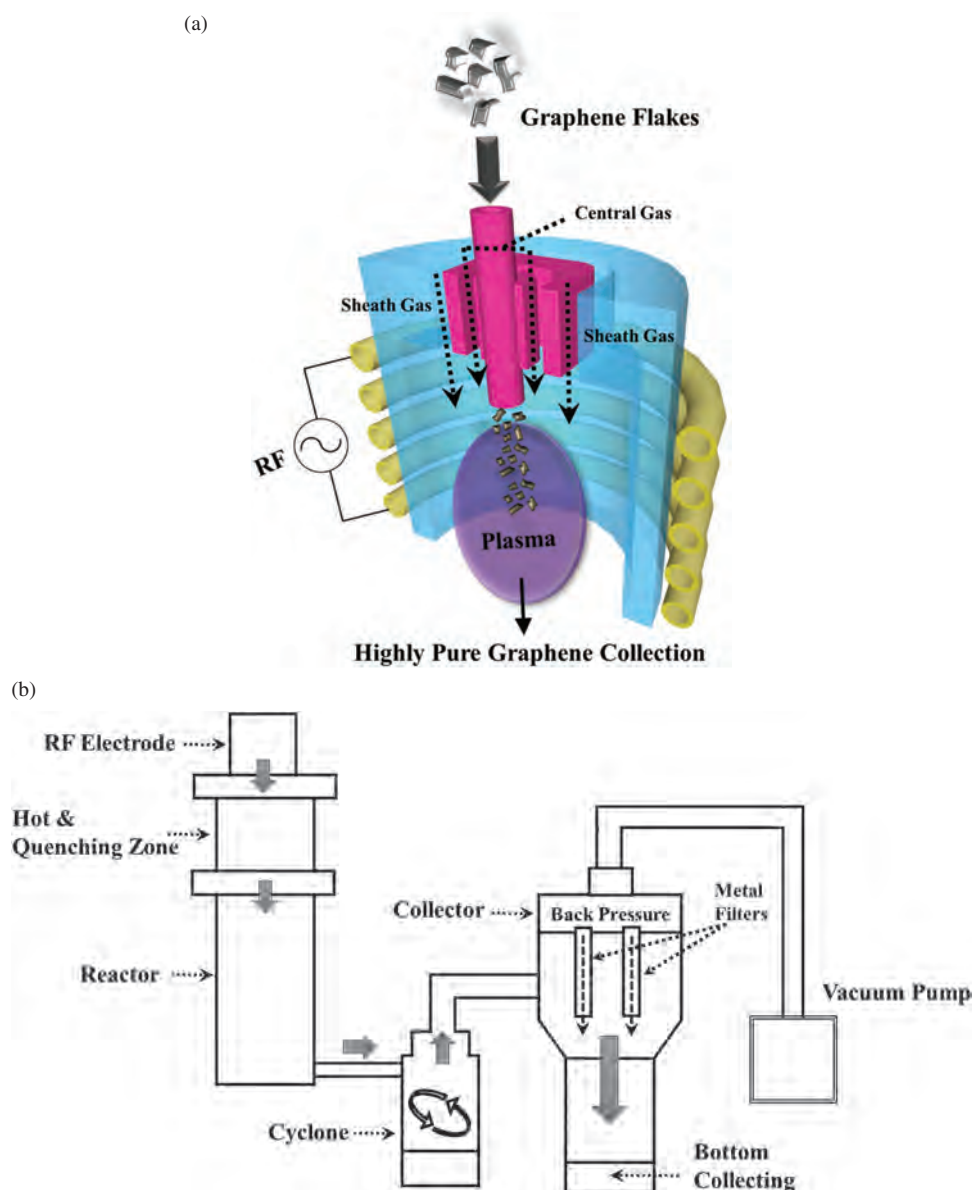


Fig. 1. (a) ICP-type Ar plasma reactor used to remove impurities on GFs. (b) Schematic diagram of the entire GF treatment system used for the removal of impurities on GFs.

during the GF feeding from the top of the reactor. The GF feeding to the chamber was carried out by flowing 10 slm of Ar with GFs. To confine the GFs in the reactor near the center of the chamber and to treat the GFs more uniformly by the plasma, the Ar gas was also flowed not only through the Ar gas feed tube (central gas) but also through a region between the chamber wall and the Ar gas feed tube (sheath gas). The central gas of about 30 slm Ar was flowed to prevent the GFs from spreading towards the chamber wall and the sheath gas of about 50 slm Ar was flowed to protect the GF spreading toward the wall further and to keep the central gas flow shape downward. Figure 1(b) shows the schematic diagram of the entire GF treatment system. The GFs treated by the plasma are fed to the collector through the cyclone. The cyclone was used to select uniform GFs by circulating the treated GFs and by removing heavy GFs to the bottom side of the cyclone. The GFs transported from the cyclone to collector are collected on the metal filters located in the collector during the vacuum pumping. The GFs collected on the metal filters are dropped to the bottom of the collector by turning off the vacuum pump and by pressurizing the metal filters.

The surface morphology of the plasma treated GFs was observed by a field emission scanning electron microscope (SEM; Hitachi S-4700) and the structural information of the GFs was investigated with Raman spectroscopy (Witec Alpha 300). The impurity of the GFs was observed using energy-dispersive X-ray spectroscopy (EDAX; Hitachi S-4700). To measure the electrical properties of the GFs, the GFs were coated on polyethylene terephthalate (PET) films by 1 cm × 1 cm using a homemade spray coating system (Spray gun; Richpen, GP-S1). Before the coating on the PET film using a spray coating system, 3 mg of the GFs was dispersed in 100 ml of isopropanol (IPA) to make a GF solution. During the coating, the substrate holder was heated at about 50 °C to vaporize the IPA on the substrate rapidly and to improve the coating uniformity. The sheet resistance of GF electrodes fabricated was measured using a 4-point probe (Changmin Tech., CMT-SR200N).

3. RESULTS AND DISCUSSION

In this study, to study the effect of Ar plasma treatment on the impurity removal of GFs, two different plasma treatment powers of 27 kW and 17 kW and two different GF feeding positions of up-state or down-state relative to the plasma generated in the reactor were used for the control of the plasma density and plasma treatment time, respectively. The impurities on GFs before and after the plasma treatments were measured by EDX and the results are shown in Figure 2 for up-state 27 kW, up-state 17 kW, and down-state 17 kW. As shown in Figure 2, for the raw GFs, about 7.7% of oxygen and 2.6% of sulfur in addition to 89.7% of carbon was observed. Therefore, for the as-received GFs, about impurities of about 10% were contained in the GFs. As shown in Figure 2, when 27 kW

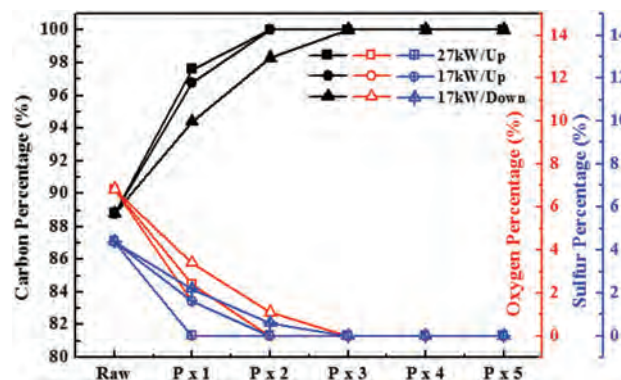


Fig. 2. The impurities in GFs before and after the plasma treatments measured by EDX. P × 1, P × 2, P × 3, P × 4, and P × 5 are the number of plasma treatment of 1, 2, 3, 4, and 5 times, respectively.

of rf power and the GF feed position of up-state were used, the sulfur was completely removed and about 4.3% of oxygen was remaining on GFs after one time of plasma treatment (P × 1). After two times of plasma treatment ($\geq P \times 2$), all the impurities were removed and pure carbon could be obtained. When the GFs were treated at a lower rf power of 17 kW and at the same GF feeding position, even though more sulfur and more oxygen were remaining on the GFs after one time treatment, all the impurities were also removed after the second treatment ($\geq P \times 2$) similar to the plasma treatment with up-state 27 kW. For the lower rf power condition of 17 kW and when the GF feeding position was changed to down-state to decrease the plasma treatment time, to remove all the impurities on the GFs, at least three times of plasma treatment ($\geq P \times 3$) was required.

The change of the GF morphology after the plasma treatments was investigated with SEM and the results are shown in Figures 3(a)–(c) for up-state 27 kW, up-state 17 kW, and down-state 17 kW, respectively. When the GFs were observed by SEM before the plasma treatment, as shown in the first figure of Figure 3, the surface of the raw GF was smooth and the size of the GF was about 5~15 μm . When the GFs were treated with 27 kW and at the up-state, as shown in Figure 3(a), even though no significant change in the surface morphology was observed after one time plasma treatment, the increase of plasma treatment time increased the defects on the GF surface by showing particle-like graphite on the surface especially after two times of plasma treatment ($\geq P \times 2$) possibly indicating significant damage of the graphene surface. When the GFs were treated by 17 kW and at the up-state, as shown in Figure 3(b), the smooth graphene surface was also observed after one time of plasma treatment, and, after two times of plasma treatment, small dust-like morphology was observed on the smooth GF surface. After three~four times of plasma treatment, significant change in the the graphene surface morphology was also observed by showing particle-shaped graphite on the graphene surface. On the contrary, when the GFs were treated with

the lower rf power of 17 kW and at the down-state, as shown in Figure 3(c), no significant change in the graphene surface morphology was observed for all of the plasma treatment conditions even though very small amount of dust-like particles were observed on the graphene surface after three times of plasma treatment. Therefore, depending on the rf power, the position of the GF feeding, and the number of the plasma treatment time, the degree of graphene surface morphology was significantly changed.

To investigate the defect formation on the GFs after the plasma treatment, the GFs were observed by Raman spectroscopy. The Raman spectroscopy of the GFs showed a

peak intensity (ID) related to the defect at near 1350 cm^{-1} , a peak more related to graphite (IG) at near 1600 cm^{-1} , and a peak more related to graphene (I2D) at near 2700 cm^{-1} . To investigate the degree of defect on the GF surface after the plasma treatment, the intensity ratios of I_D/I_G were measured and the results are shown in Figure 4. As shown in Figure 4, after the one time plasma treatment, the intensity ratios of I_D/I_G were slightly decreased for all of the plasma treatment conditions showing no significant change in the graphene surface morphology as observed by SEM in Figure 3 indicating the improvement of graphene properties possibly due to the removal of loosely bound

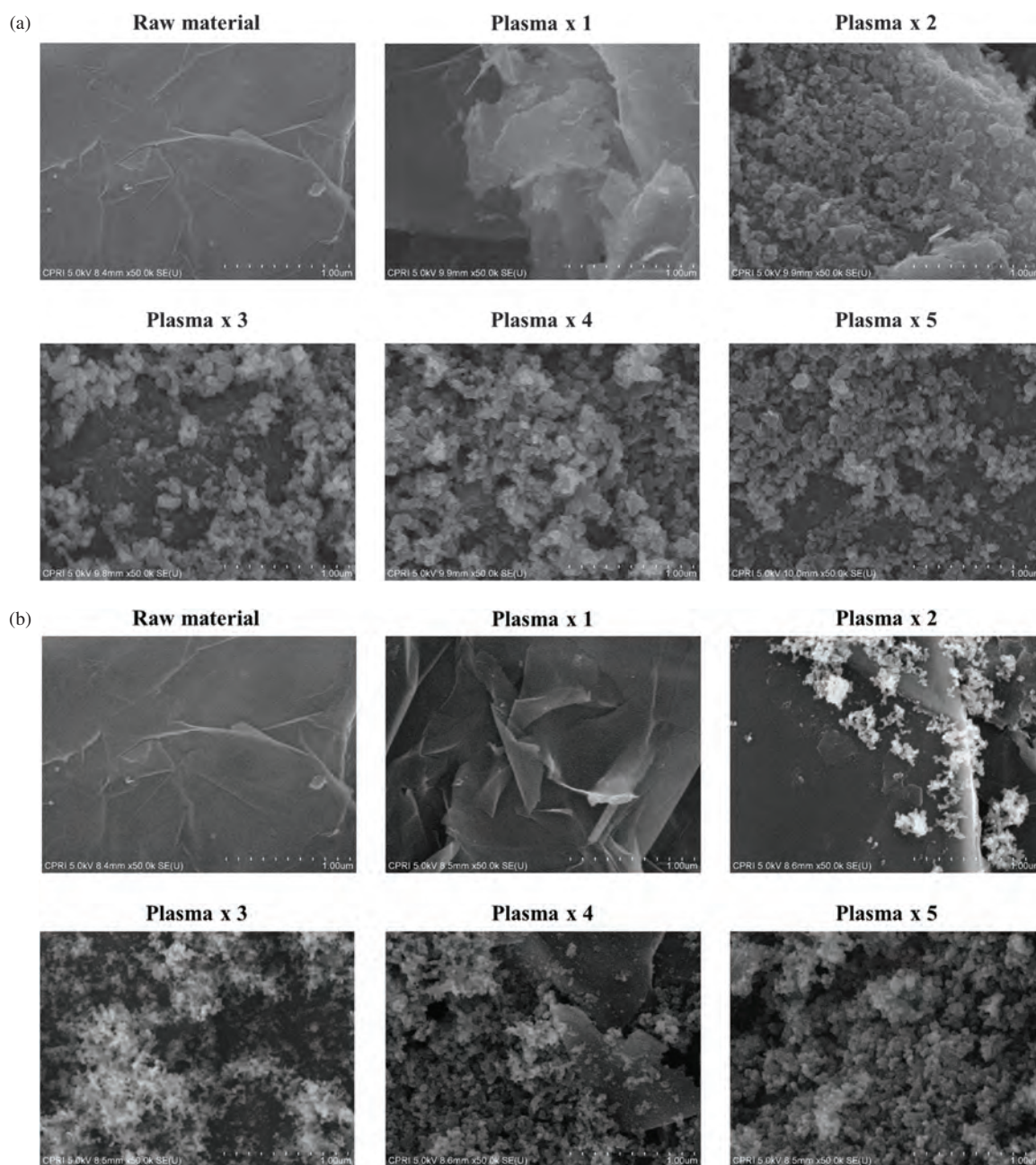


Fig. 3. Continued.

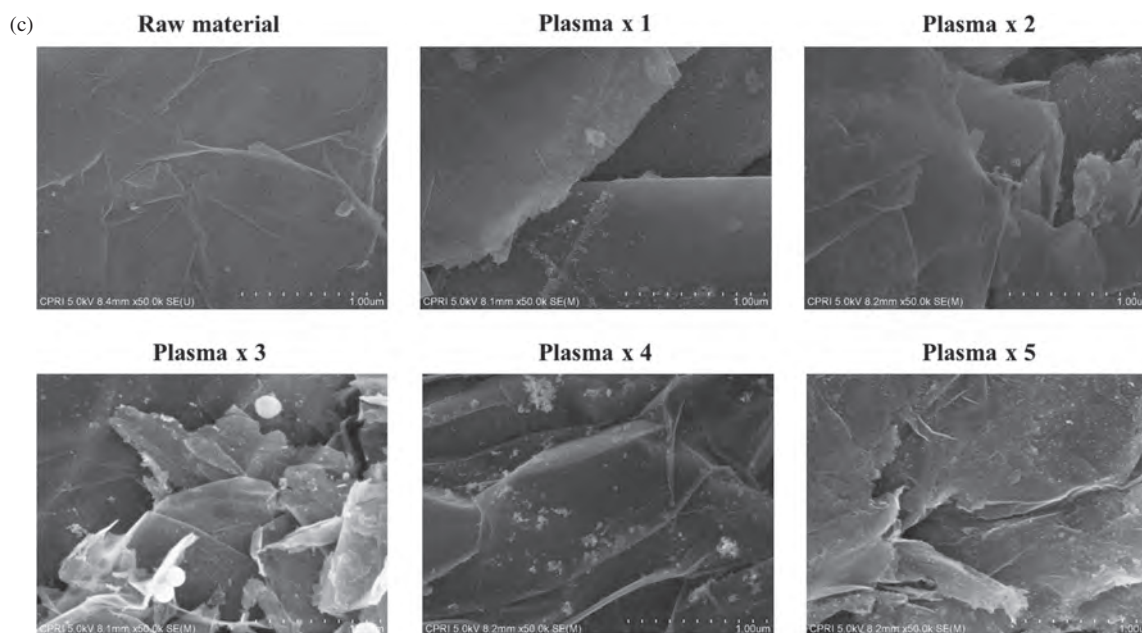


Fig. 3. (a) SEM micrographs of GFs observed before and after the plasma treatments (1~5 times) with 27 kW of rf power and at the GF feeding position of up-state. (b) SEM micrographs of GFs observed before and after the plasma treatments (1~5 times) with 27 kW of rf power and at the GF feeding position of down-state. (c) SEM micrographs of GFs observed before and after the plasma treatments (1~5 times) with 17 kW of rf power and at the GF feeding position of down-state.

carbon, oxygen, and sulfur on the surface. However, for the up-state 27 kW, possibly due to the significant defect formation on the graphene surface as observed by the formation of particle-like graphite in Figure 3(a), the ratio of I_D/I_G was increased significantly with the increase of plasma treatment time when the plasma treatment time was further increased. In the case of up-state 17 kW, due to the lower Ar plasma density, the I_D/I_G was more slowly increased with the further increase of plasma treatment time ($\geq P \times 2$) compared with those for 27 kW. On the contrary, the use of 17 kW and down-state decreased the I_D/I_G with the further increase of plasma treatment time up to five times of plasma treatment indicating the decrease of defect formation on the surface (or, at least, no increase of defect on the graphene surface by the plasma treatment because the decrease of I_D/I_G with the plasma treatment can be also related to the removal of loosely bound carbon on the graphene surface). Therefore, using the plasma treatment of the GFs for more than three times with 17 kW and at the down-state, not only the 100% removal of impurities such as oxygen and sulfur on the GFs but also the decrease of possible defects (or no increase of physical damage) on the graphene surface could be observed.

The raw GFs and the plasma treated GFs were sprayed on the PET substrates using a spray coating system as explained in the experimental section and the sheet resistance of the GF films on the PET substrate was measured using a 4-point probe and the results are shown in Figure 5. As shown in Figure 5, for the up-state 27 kW, even though the sheet resistance was slightly decreased after one time

plasma treatment possibly due to the decrease of impurities such as oxygen and sulfur and due to the decrease of surface defect, the further increase of plasma treatment time increased the sheet resistance significantly from about 1000 Ω/sq (raw GFs) to about 5000 Ω/sq after five times of plasma treatment due to the significant defect formation on the graphene surface. The use of 17 kW and up-state also increased the sheet resistance with the increase of plasma treatment time but the increase of sheet resistance after the same plasma treatment time was lower (about 3,200 Ω/sq after five times of plasma treatment) compared to the condition of 27 kW and up-state possibly due to the smaller defect formation on the graphene surface at the

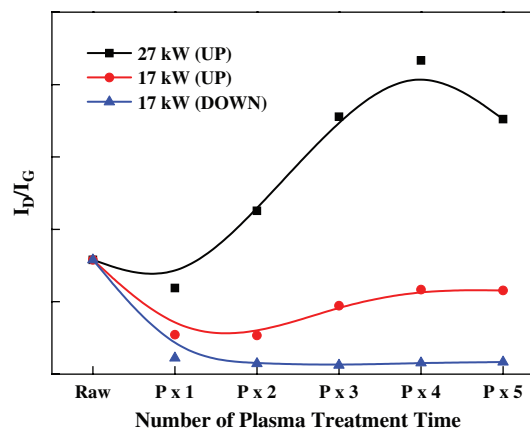


Fig. 4. Raman intensity ratios of I_D/I_G measured to investigate the degree of defects on the GF surface after the various plasma treatments.

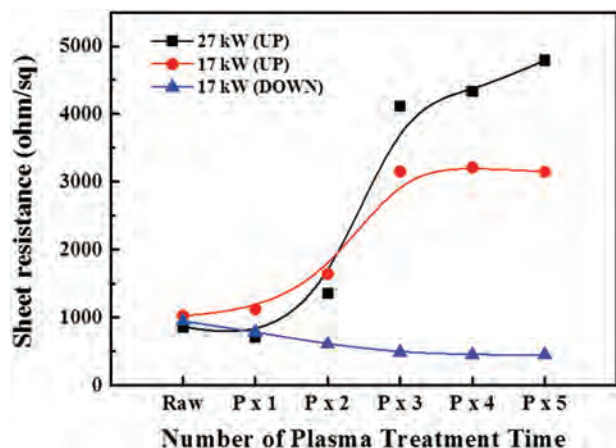


Fig. 5. Sheet resistance of the GF films on the PET substrate measured using a 4-point probe for the raw GFs and the plasma treated GFs sprayed on the PET substrates using a spray coating system.

lower rf power. However, when the GFs were treated with 17 kW and down-state, the sheet resistance was continuously decreased with the increase of plasma treatment time by decreasing to about 450 Ω/sq , therefore, about 50% of decrease in sheet resistance after five times of plasma treatment due to the complete removal of impurities in addition to the decrease of surface defects (or at least no increase of surface defects) on the graphene surface.

4. CONCLUSION

The GFs containing impurities such as oxygen and sulphur were treated with various conditions of ICP-type Ar rf plasmas and the effect of the rf plasma treatment on the removal of the impurities, the change of defect, and the change of surface morphology was investigated. Also, the sheet resistances of the plasma treated GFs sprayed on the PET substrates were also investigated. After the plasma treatment of GFs, that is, by passing through the Ar plasma area, the impurities such as oxygen and sulphur were completely removed after one or two times of plasma treatment. The higher rf power of 27 kW compared to 17 kW and the use of up-state instead of down-state decreased the impurities faster due to the higher plasma density and longer plasma exposure time. However, the use of the higher rf power and the use of up-state generally increased the defects on the graphene surface as observed by SEM as the particle-like graphite and as measured by the increased I_D/I_G with Raman spectroscopy. Especially, by using the lower rf power of 17 kW and the down-state of GF feeding for the GF treatment, no defect formation was observed with the increase of plasma treatment time indicating no change (or decrease of defect) on the graphene surface in addition to the removal of impurities. When the sheet resistances of GF electrodes were measured, the GFs treated with 17 kW and down-state showed the continuous decrease of sheet resistance to about 50% with the increase of plasma treatment time to five times

while the other conditions of higher rf power and up-state increased the sheet resistance with the increase of plasma treatment time. Therefore, by using an appropriate ICP-type Ar plasma treatment, the improvement of GF quality such as the decrease of impurities, the decrease of defects, and the lower electrical resistance could be achieved at large quantities.

Acknowledgments: This work was supported by the Industrial Strategic Technology Development Program (10041681, Development of fundamental technology for 10 nm process semiconductor and 10 G size large area process with high plasma density and VHF condition) funded by the Ministry of Knowledge Economy (MKE, Korea). And this work was also supported by the Industrial Strategic technology development program (10041926, Development of high density plasma technologies for thin film deposition of nanoscale semiconductor and flexible display processing) funded by the Ministry of Knowledge Economy (MKE, Korea).

References and Notes

1. A. K. Geim and K. S. Novoselov, *Nat. Mater.* 6, 183 (2007).
2. K. S. Novoselov, A. K. Geim, S. V. Morozov, D. Jiang, M. I. Katsnelson, I. V. Grigorieva, S. V. Dubonos, and A. A. Firsov, *Nature* 438, 197 (2005).
3. A. A. Balandin, S. Ghosh, W. Bao, I. Calizo, D. Teweldebrhan, F. Miao, and C. N. Lau, *Nano Lett.* 8, 902 (2008).
4. C. Lee, X. Wei, J. W. Kysar, and J. Hone, *Science (New York, N.Y.)* 321, 385 (2008).
5. X. Li, W. Cai, J. An, S. Kim, J. Nah, D. Yang, R. Piner, A. Velamakanni, I. Jung, E. Tutuc, S. K. Banerjee, L. Colombo, and R. S. Ruoff, *Science (New York, N.Y.)* 324, 1312 (2009).
6. K. S. Kim, Y. Zhao, H. Jang, S. Y. Lee, J. M. Kim, K. S. Kim, J.-H. Ahn, P. Kim, J.-Y. Choi, and B. H. Hong, *Nature* 457, 706 (2009).
7. A. Reina, X. Jia, J. Ho, D. Nezich, H. Son, V. Bulovic, M. S. Dresselhaus, and K. Jing, *Nano Lett.* 9, 30 (2009).
8. M. Wang, S. K. Jang, W. J. Jang, M. Kim, S. Y. Park, S. W. Kim, S. J. Kahng, J. Y. Choi, R. S. Ruoff, Y. J. Song, and S. Lee, *Adv. Mater.* 25, 2746 (2013).
9. M. Losurdo, M. M. Giangregorio, P. Capezzuto, and G. Bruno, Graphene CVD Growth on Copper and Nickel: Role of Hydrogen in Kinetics and Structure (2011).
10. B. Jayasena and S. Subbiah, *Nanoscale Research Letters* 6, 95 (2011).
11. Y. Hernandez, V. Nicolosi, M. Lotya, F. M. Blighe, Z. Sun, S. De, I. T. McGovern, B. Holland, M. Byrne, Y. K. Gun'ko, J. J. Boland, P. Niraj, G. Duesberg, S. Krishnamurthy, R. Goodhue, J. Hutchison, V. Scardaci, A. C. Ferrari, and J. N. Coleman, *Nat. Nanotechnol.* 3, 563 (2008).
12. L. Zhu, X. Zhao, Y. Li, X. Yu, C. Li, and Q. Zhang, *Mater. Chem. Phys.* 137, 984 (2013).
13. M. Yi, Z. Shen, S. Ma, and X. Zhang, *J. Nanopart. Res.* 14 (2012).
14. M. Lotya, Y. Hernandez, P. J. King, R. J. Smith, V. Nicolosi, L. S. Karlsson, F. M. Blighe, S. De, W. Zhiming, I. T. McGovern, G. S. Duesberg, and J. N. Coleman, *J. Am. Chem. Soc.* 131, 3611 (2009).
15. H. Wang, J. T. Robinson, X. Li, and H. Dai, *J. Am. Chem. Soc.* 131, 9910 (2009).
16. M. Choucair, P. Thordarson, and J. A. Stride, Gram-Scale Production of Graphene Based on Solvothermal Synthesis and Sonication (2009).

17. L. Huang, B. Wu, J. Chen, Y. Xue, D. Geng, Y. Guo, G. Yu, and Y. Liu, *Small* 9, 1330 (2013).
18. N. Li, Z. Wang, K. Zhao, Z. Shi, Z. Gu, and S. Xu, *Carbon* 48, 255 (2010).
19. X. Huang, X. Qi, F. Boey, and H. Zhang, Graphene-Based Composites (2012).
20. T. Kuilla, S. Bhadra, D. Yao, N. H. Kim, S. Bose, and J. H. Lee, Recent Advances in Graphene Based Polymer Composites (2010).
21. M. A. Rafiee, W. Lu, A. V. Thomas, A. Zandiatashbar, J. Rafiee, J. M. Tour, and N. A. Koratkar, *ACS Nano* 4, 7415 (2010).
22. J. Liang, Y. Wang, Y. Huang, Y. Ma, Z. Liu, J. Cai, C. Zhang, H. Gao, and Y. Chen, Electromagnetic Interference Shielding of Graphene/Epoxy Composites (2009).
23. J. K. Lee, K. B. Smith, C. M. Hayner, and H. H. Kung, *Chemical Communications (Cambridge, England)* 46, 2025 (2010).
24. E. J. Yoo, J. Kim, E. Hosono, H. S. Zhou, T. Kudo, and I. Honma, *Nano Lett.* 8, 2277 (2008).
25. H. Wang, L.-F. Cui, Y. Yang, H. Sanchez Casalongue, J. T. Robinson, Y. Liang, Y. Cui, and H. Dai, *J. Am. Chem. Soc.* 132, 13978 (2010).
26. Y. Wang, Z. Shi, Y. Huang, Y. Ma, C. Wang, M. Chen, and Y. Chen, *Journal of Physical Chemistry C* 113, 13103 (2009).
27. C. Liu, Z. Yu, D. Neff, A. Zhamu, and B. Z. Jang, *Nano Lett.* 10, 4863 (2010).
28. K. Zhang, L. L. Zhang, X. S. Zhao, and J. Wu, *Chem. Mater.* 22, 1392 (2010).
29. L. L. Zhang, R. Zhou, and X. S. Zhao, Graphene-Based Materials as Supercapacitor Electrodes (2010).
30. S. H. Huh, *Engineering and Technology* 73 (2010).
31. S. Pei and H. M. Cheng, The Reduction of Graphene Oxide (2012).
32. S. Stankovich, D. A. Dikin, R. D. Piner, K. A. Kohlhaas, A. Kleinhammes, Y. Jia, Y. Wu, S. T. Nguyen, and R. S. Ruoff, *Carbon* 45, 1558 (2007).
33. W. Chen, L. Yan, and P. R. Bangal, *Carbon* 48, 1146 (2010).
34. M. J. Kim, Y. Jeong, S. H. Sohn, S. Y. Lee, Y. J. Kim, K. Lee, Y. H. Kahng, and J. H. Jang, *AIP Advances* 3, 0 (2013).
35. S. W. Lee, C. Mattevi, M. Chhowalla, and R. M. Sankaran, *Journal of Physical Chemistry Letters* 3, 772 (2012).